match no. 29 pp. 107-130 1993

THE FRACTAL FAMILY OF CORO[N]ENES

D. J. Klein, T. P. Živković[1] and A. T. Balaban[2]
Department of Marine Sciences
Texas A&M University at Galveston
Galveston, Texas 77553-1675

(Received September 1992)

ABSTRACT

A novel self-similar sequence of aromatic hydrocarbons beginning with benzene and coronene is proposed. The asymptotically fractal character of the resultant multi-coronoid species is pointed out and some consequences are elaborated upon. Kekulé structures are enumerated, and the proton-NMR and C-H stretching spectra are discussed at a qualitative level, whence it is argued that fractality should emerge in these spectra.

1. Permanent address: Ruder Bošković Institute, 41001 Zagreb, Croatia.
2. Permanent address: Dept. of Organic Chemistry, Polytechnic Institute, Bucharest, Roumania.

1. Introduction

Benzenoid species in a broad sense offer a rich range of structures entailing delocalized chemical bonding. The journal Polycyclic Aromatic Compounds is devoted to these species, the journal Carbon is in fact dominated by studies of aromatic carbonaceous materials, the new journal Buckminsterfullerene Science and Technology may be viewed as devoted to a special subclass of these species, and general organic chemistry journals continue to have a notable fraction of their volume devoted to this subject. Of the species in this broad area the sequence beginning with benzene, coronene and Kekulene, as in figure 1, has served as one focal within this field. The higher members are[1] the hexagonal coronoids.

Here we study another sequence beginning with benzene and coronene, and the $(n+1)^{th}$ member related to the n^{th} in much the same way as coronene is related to benzene. The first four members of this sequence are indicated in figure 2. Identifying benzene and coronene as the n=0 and n=1 members, we propose that the n=2 and n=3 members be dubbed coro-coronene and coro-coro-coronene, while the general n^{th} member is coro$^{(n)}$ene. In fact, this notably "self-similar" sequence develops toward a so-called[2] fractal limit, such as we have discussed different cases of previously[3]. One feature of such a sequence is that the mass (or molecular weight) scales as a characteristic length raised to a fractional power d, which may be interpreted as a geometric dimension, here called the fractal dimension. In section 2 this is discussed further, whence we find

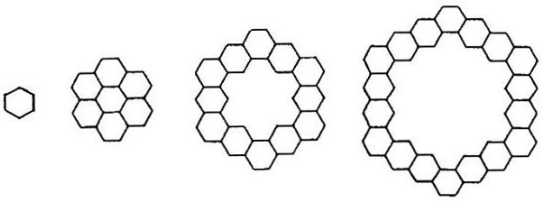

Figure 1 - The first four members of a focal sequence of hexagonal structures.

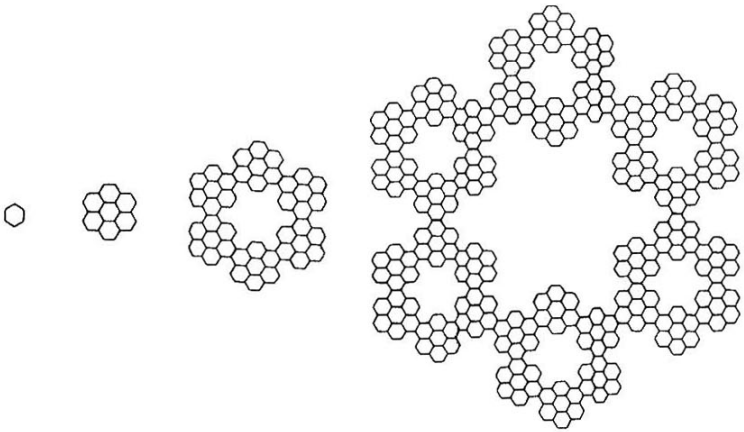

Figure 2 - The first four members (with n=0,1,2,3) of a self-similar sequence of coro[n]ene structures. Note that their sizes (measured by their numbers of C-atoms) increases exponentially with n.

$d \approx 1.63093$. The aromatic character of the members of such a sequence is also of interest, and is studied here in section 3 via an enumeration of each member's Kekulé structures. This indicates that quite rapidly the resonance energy per site approaches a limit, but only slightly different than that of coronene. In section 4 we consider the manner in which the fractal molecular structure can be expected to perturb localized spectral features such as H-NMR or ^{13}C-NMR chemical shifts or coupling constants or C-H stretching frequencies. The self-similar molecular structure is argued to implicate a heirarchy of spectral splittings of ever diminishing scales, so that the consequent spectrum itself takes on a self-similar character, with a fractal dimension which is a fraction of that associated to the molecular structure.

2. Simple Structural Features

Many structural features of the sequence of coro$^{[n]}$enes are revealed from a study of the construction leading from one stage to the subsequent one. Indeed we may view the $(n+1)^{th}$ stage as being constructed by the fusion of six n^{th} stage species, as in figure 3. In any single fusion two neighbor pairs of C-atoms are merged into a single neighbor pair. Thence letting γ_n denote the number of C-atoms in the n^{th} stage species and noting that there are six fusions in figure 3, we see that

$$\gamma_{n+1} = 6\gamma_n - 6*2 \tag{2.1}$$

Similarly if we note that four hydrogens are lost at each fusion, then with η_n denoting the number of H-atoms at the n^{th} stage we have

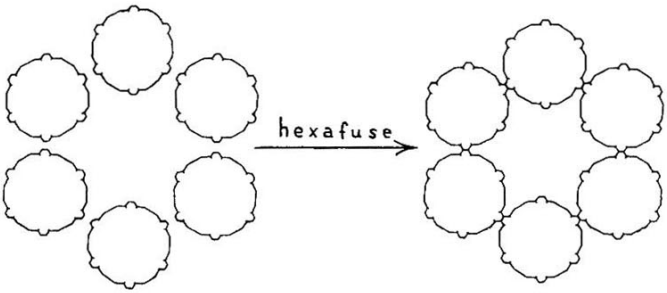

Figure 3 - The manner of combination of six coro[n]enes to yield the next stage coro[n+1]ene.

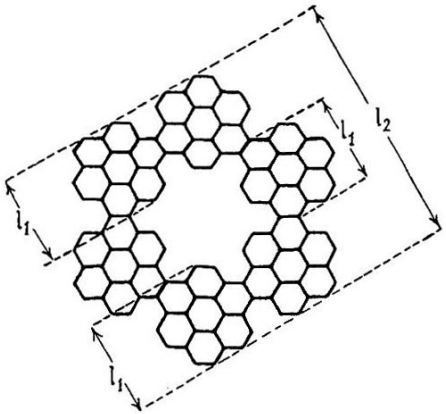

Figure 4 - Illustration of the length-recursion relation of eqn. (2.3) for n=2.

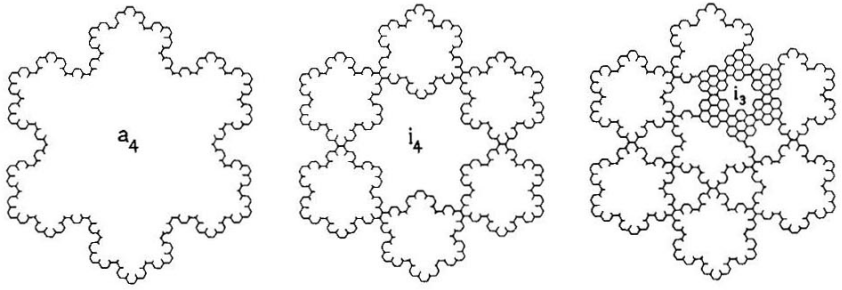

Figure 5 - Illustration of areas involved in eqns. (2.6) and (2.7) for n=2. The relation between the first and second structures illustrates (2.6), while the relation between the second and third illustrates (2.7).

(2.2) $$\eta_{n+1} = 6\eta_n - 6\times 4$$

Further we let l_n be the n^{th} stage "molecular span" measured as the distance between two minimally separated parallel lines fully enclosing an n^{th} stage diagram. As illustrated in figure 4 the span at stage n+1 is but a slight correction to three n^{th} stage spans (for $n\geq 1$),

(2.3) $$l_{n+1} = 3l_n - 2\times(\tfrac{1}{2})$$

where we assume perfect hexagons and choose the unit of length to be that of the C-C bonds. The length p_n of the outer periphery of an n^{th} stage species is nearly 6 times 2/3 of that for the preceding stage, except that for each fusion one bond length is lost, so that

(2.4) $$p_{n+1} = 4p_n - 6$$

Readily one sees that the number of hexagonal rings in the $(n+1)^{th}$ stage is

(2.5) $$h_{n+1} = 6h_n$$

so long as $n\geq 1$, the exceptional relation $h_1 = 7h_0$ applying (unless one were not to count the hexagon in the center of a coronene).

The recursion for the area enclosed in the outer periphery needs a little more explanation. If we denote this area for an n^{th} stage molecule by a_n and the area enclosed in the center by i_n then it is clear that

(2.6) $$a_{n+1} = 6a_n + i_{n+1}$$

and the problem devolves to a recursion for the inner area. Now one n^{th} stage gasket can be fit in the center of an $(n+1)^{th}$ stage one usisng edge fusions and leaving six remnant empty areas, as indicated in figure 5. Examination reveals each such empty area is

surrounded by six $(n-1)^{th}$ gaskets so that each empty area is that in the center of an n^{th} stage gasket. That is

(2.7) $$i_{n+1} = a_n + 6i_n$$

Thence we have a pair of coupled recursions.

All the recursions are in essence of a straightforward type. They typically are of the form

(2.8) $$x_{n+1} = Ax_n + b$$

and have solutions

(2.9) $$x_n = A^n\alpha + \beta$$

$$\alpha = A^{-1}(x_e - \beta)$$

$$\beta = (1-A)^{-1}b$$

where x_e is some (usually small-gasket with e=0 or 1) initial condition. The recursion for areas may be brought into the desired form of (2.8) if we substitute (2.7) into (2.6) and write the result along with (2.7) as

(2.10) $$\begin{pmatrix} a_{n+1} \\ i_{n+1} \end{pmatrix} = \begin{pmatrix} 7 & 6 \\ 1 & 6 \end{pmatrix} \begin{pmatrix} a_n \\ i_n \end{pmatrix}$$

Of course x_{n+1}, x_n and b in (2.8) are now interpreted as column vectors (with b=0) and A as a 2 by 2 matrix, but still the solution of (2.9) applies (with the ordering of the different factors now crucial). Thus we have

$$
\left.\begin{aligned}
\gamma_n &= \frac{18}{5}6^n + \frac{12}{5} \\
\eta_n &= \frac{6}{5}6^n + \frac{24}{5} \\
p_n &= 4^{n+1} + 2
\end{aligned}\right\} \quad n \geq 0
$$

(2.11)

$$
\left.\begin{aligned}
l_n &= \frac{3}{2}3^n + \tfrac{1}{2} \\
h_n &= 7 \times 6^{n-1} \\
a_n &= \frac{3}{5}9^n + \frac{2}{5}4^n \\
i_n &= \frac{1}{5}9^n - \frac{1}{5}4^n
\end{aligned}\right\} \quad n \geq 1
$$

where in the last two equations the areas are in units of a single hexagon (and l_n is in units of bond lengths). Moreover the molecular weight is $M_H\eta_n+M_C\gamma_n$ where M_H and M_C are the atomic weights for H- and C-atoms.

Various asymptotic properties of the fractal limit may now be identified. Most simply the ratio of hydrogen to carbon approaches a constant value

$$\lim_{n\to\infty} \eta_n/\gamma_n = \tfrac{1}{3}$$

Of more present interest is the (mass-based) fractal dimension

$$d = \lim_{n\to\infty} \frac{\ln(M_H\eta_n+M_C\gamma_n)}{\ln l_n} = \frac{\ln 6}{\ln 3} \approx 1.63093$$

Notice that this does not depend on the values of the atomic

weights (even if the species were to be perfluorinated). Nor does it depend upon our particular choice of characteristic length —which we could also take as the maximum distance between two points on the molecular diagram, or as the mass-weighted mean radius of gyration. Thence d represents a "pure" structural characteristic. In fact d is not altered if we initiate the growth procedure with a seed of hexagonal symmetry other than benzene: starting with coronene merely shifts the stage numbers by 1, but starting e.g. with Kekulene (of figure 1) initiates a whole new family. Evidently too the outer periphery is fractal with another dimension

$$d_p = \lim_{n\to\infty} \frac{\ln p_n}{\ln l_n} = \frac{ln4}{ln3} \approx 1.26186$$

Indeed this is exactly the fractal dimension of the boundary of the hexagonal "Koch snowflake", which entails a related construction. See, e.g., pages 42 and 43 of reference 2.

3. Kekulé Structure Enumeration

Kekulé-structure counts are often deemed a reasonable indicator of resonance energy. Thence these counts for the coro[n]-enes are of interest. This can be accomplished via recursions reminescent of those of the last section but more involved. Indeed we utilize several "auxiliary" counts for subclasses of Kekulé structures with fixed arrangements of (double) bonds at the pairs of neighbor sites where fusion may take place. There are five such

patterns as shown (and named) in figure 6. Then we define $K_n(x,y,z)$ to be the number of perfect pairings (i.e., Kekulé structures) possible within an n^{th} stage gasket if there are local arrangements x, y, z at each of the potential points of fusion, as indicated in figure 3. A diagrammatic notation is convenient

(3.1)

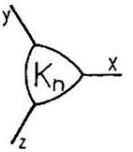

$\equiv K_n(x,y,z)$

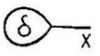

$\equiv \delta(x,0) + \delta(x,\omega)$

and if we had a quantity doubly indexed by the local arrangements, it would be represented by a "pod" with two dangling lines. Joining two dangling lines while removing their labels indicates a summation

(3.2)

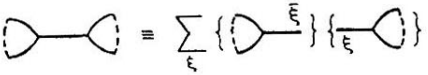

where ξ denotes the local arrangement needed to accomplish fusion of one fragment to another when the other has local arrangement ξ. That is,

(3.3) $\quad \bar{\omega} = \tilde{\omega}\,, \tilde{\bar{\omega}} = \omega,\ \bar{0} = 0,\ \bar{\varepsilon} = \varepsilon,\ \bar{\varepsilon}' = \varepsilon$

Then one readily sees the recursion

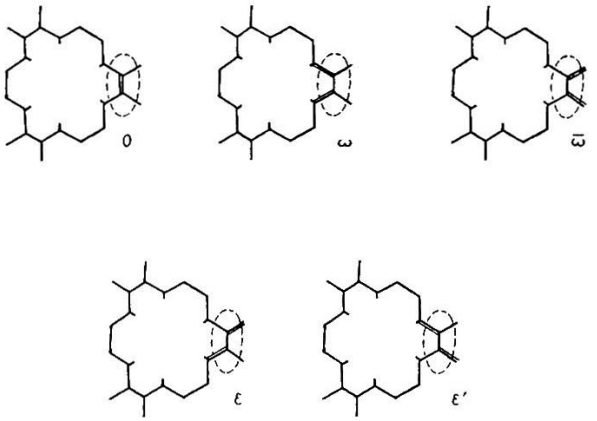

Figure 6 - The five local patterns of π-bonds at the location of a fusion (as encircled here by a dashed line).

(3.4)

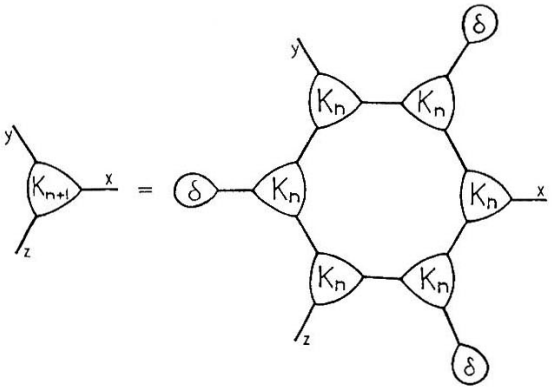

in close correspondence to the construction of figure 3. Further one sees that the total Kekulé-structure count for coro[n]ene is

(3.5)

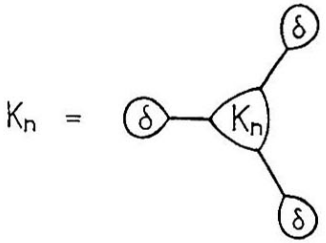

as is desired.

Perhaps a digression is in order concerning the computational efficacy of our scheme. Eqn.(3.4) applies for 5^3=125 quantities at each stage (as one varies x, y, z) while for each of the 9 internal bond there is an independent 5-fold summation thereby leading to a $5^9 \approx 2\ 10^6$ fold overall summation. Thence the iteration can be somewhat time consuming unless one takes at least one of several (easy) steps to accelerate the process. Perhaps the most significant is to introduce a second auxiliary array

(3.6)

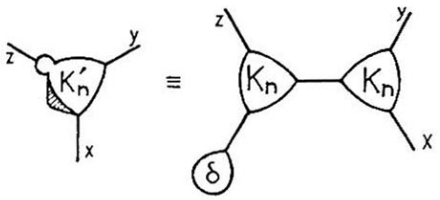

which entails a 5^2-fold overall summation for 5^3 quantities. Then instead of (3.4) utilize

(3.7)

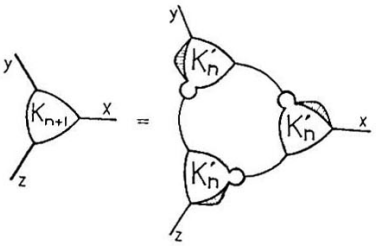

which entails an overall 5^3-fold summation for 5^3 quantities, with effort here added to (rather than multiplied by) the effort entailed in (3.5). Further one could make use of the 3-fold (rotational) symmetry in the $K_n(x,y,z)$, and also not sum over zeroes. (Since the local states ε and ε' can only occur when the other does, there are 80 of the $K_n(x,y,z)$ that must be 0.)

We have implemented the iterative scheme outlined here to obtain the results of table I. Clearly the asymptotic value of the per-site Kekulé structure count

$$\lim_{n\to\infty} K_n^{1/\gamma_n} \approx 1.143320 \tag{3.8}$$

is quickly approached very closely. Of course the molecular gaskets also grow very rapidly in size so that at stage n=12 it should be about 0.1 mm in diameter. Corresponding to the per-site Kekulé structure count we also anticipate the resonance energy per site to quickly approach its asymptotic value. That is, if we make the approximation

Table I –Kekulé-structure Enumerations

n	γ_n	$K_n/10^x$	x	K_n^{1/γ_n}
0	6	2.00000	0	1.122462
1	24	2.40000	1	1.132947
2	282	3.77181	7	1.141295
3	1680	1.85903	45	1.142977
4	10068	2.66638	271	1.143263
5	60396	2.32131	1628	1.143311
6	362364	1.01064	9770	1.143319
7	2174172	6.8830	58619	1.143320
8	13045020	6.8684	351718	1.143320
9	78270108	6.7818	2110312	1.143320
10	469620636	6.285	12661876	1.143320
11	2817723804	3.980	75971260	1.143320
12	16906342812	2.57	455827563	1.143320

(3.9) $$RE_n \approx A \ln K_n$$

as is reasonable[4] for Kekulé-structure rich benzenoids, then

$$\lim_{n\to\infty} RE_n/\gamma_n\epsilon_g \approx 0.829$$

where $\epsilon_g \approx 0.212$eV. is the asymptotic (per site) value[5] for graphite. This is higher than the corresponding ratio of 0.715 for benzene, or of 0.773 for coronene.

4. Fractal Perturbation

The question naturally arises as to how the fractal character of the coro[n]enes might be manifested in their NMR or IR spectra. An answer to a related question is indicated by Alexander and Orbach[6] who consider regular fractal structures with all bonds equivalent which in the large-gasket limit give rise to a fractal-characterized low-frequency vibrational (i.e. phonon) spectrum. Their ideas do not directly carry over to the C-C bond stretching vibrational spectrum because there is generally some complication due to double-bond localization as governed by resonance, as in the preceding section. Here we consider a different problem as concerns the effects of the fractality in perturbing a localized spectral feature such as the frequency of the proton- or carbon-13-NMR chemical shifts or vibrational CH-stretching frequencies.

The question of H-NMR chemical shifts relates to equivalence classes of H-atoms. For a coro[n]ene the global symmetry is D_{6h} with no H-atom left fixed by any symmetry elements other than the

reflection σ_h and the identity 1. Thus there are 12 H-atoms in each (global symmetry) equivalence class of which there must be $\eta_n/12$ (where as in section 2 η_n is the number of H-atoms at the n^{th} stage). But these global equivalence classes tell little about the extent of inequivalence (or frequency shifting), this being more fully addressed if one considers "local" equivalence classes. At the local extreme of just focusing on single hexagons, one sees that every H-atom is in a hexagon with but one other H-atom at a nearest-neighbor position so that at this extreme there is but a single equivalence class.

Between the global and local extremes of the previous paragraph one may look at intermediate stage equivalences. We define two H-atoms as m-equivalent if they are in like environments within an m^{th} stage component (of an n^{th} stage gasket with $n \geq m$). Thence $m=0$ and $m=n$ correspond to the two extremes already discussed. There are secondary and tertiary n^{th} stage components (or m-gaskets) attached to either 2 or 3 other such m-gaskets. Evidently the η_m-4 and η_m-6 H-atoms of these two respective types of m-gaskets belong to disjoint sets of m-equivalence classes (or m-classes) to which we may then also apply the adjectives "secondary" and "tertiary". A secondary gasket has local C_{2v} symmetry (the σ_h element of which leaves H-atoms fixed) so that its H-atoms fall into $(\eta_m-4)/2$ m-classes. Similarly the D_{3h} local symmetry of a tertiary gasket leads to $(\eta_m-6)/6$ m-classes. Thus we have a total of

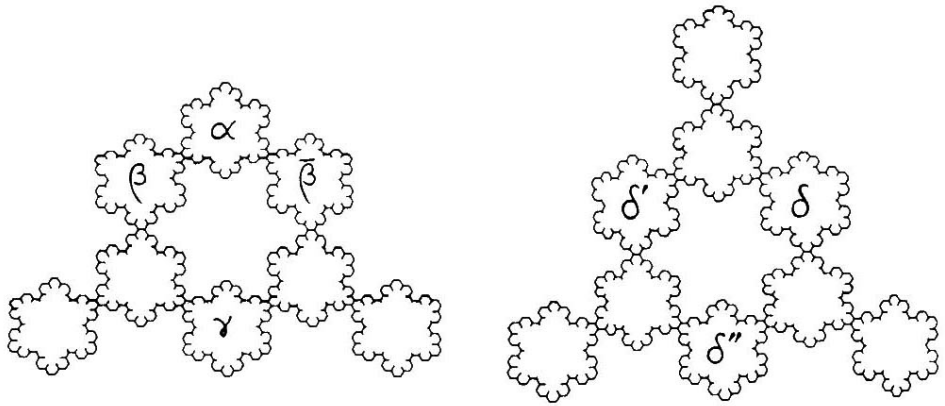

Figure 7 - Secondary (in a) and tertiary (in b) m+1-gaskets showing the four types of m-gaskets under m+1-equivalence. Here β and $\bar{\beta}$ are m+1-equivalent. Also δ, δ' and δ'' are m+1-equivalent.

$$\frac{\eta_m-4}{2} + \frac{\eta_m-6}{6} = \frac{2\eta_m-9}{3} = \frac{4}{5}6^m + \frac{1}{5}$$

m-classes. Further if we define s_{mn} and t_{mn} as the numbers of secondary and tertiary m-gaskets in coro$^{[n]}$ene, then we see that each secondary m-class contains $2s_{mn}$ H-atoms, while there are $6s_{mn}$ H-atoms in each tertiary case.

Spectral splitting patterns turn out to be related to equivalence class splittings, so that the splitting of m-classes into m+1-classes is of interest. For instance, secondary m-gaskets, which of course are all m-equivalent, are no longer m+1-equivalent and indeed fall into m+1-equivalence types associated to α, β, γ, δ. But there may be some further splitting if symmetry of an m-gasket is lowered on extending consideration to its location in its m+1-gasket. Thus the m+1-classes arising from β (or $\beta \cup \beta$) split in two, while those from δ(or $\delta \cup \delta' \cup \delta''$) split in three. So letting Λ be a label for a secondary m-class we see that it splits into m+1-classes as

(4.2) $\quad C_\Lambda = C_{\Lambda\alpha} \cup C_{\Lambda\beta 1} \cup C_{\Lambda\beta 2} \cup C_{\Lambda\gamma} \cup C_{\Lambda\delta 1} \cup C_{\Lambda\delta 2} \cup C_{\Lambda\delta 3}$

That is, each secondary m-class splits into 4 secondary and 3 tertiary m+1-classes. This and the corresponding (similarly derived) result for the splitting of tertiary m-classes might be abbreviated

(4.3) $\quad$ *sec.-m* $\rightarrow$ *4 sec.-m+1* $\cup$ *3 tert.-m+1*

tert.-m $\rightarrow$ *2 sec.-m+1* $\cup$ *3 tert.-m+1*

That is, the second of these relations tells us a tertiary m-class

splits into 2 secondary and 3 tertiary m+1-classes.

We now seek a qualitative description of the spectral splittings. Imagine that for a given spectral resolution only interactions over m^{th} stage gaskets are relevant but that for an increased resolution interactions over $(m+1)^{th}$ stage gaskets are relevant. Then one anticipates via (4,3) that a "secondary" lower-resolution spectral line will split into 4 secondary and 3 tertiary spectral lines as one proceeds to the higher resolution. Similarly also via (4.3) each tertiary lower-resolution line should split into 2 secondary and 3 tertiary spectral lines. Further this manner of splitting should repeat on proceeding to even higher resolution. Moreover, the splitting patterns should be the same except for scale. The change in scale is related to the asymptotic form of the interaction strength, say $-l^{-a}$ for two sites a distance l apart (where, e.g., a=3 for dipole-dipole-like interactions). Thence if we let Δ_m be the splitting magnitude due to interactions over a length l_m characterizing an m-gasket, then upon recalling (2.3), we see that

$$\Delta_{m+1} \approx \Delta_m/3^a \tag{4.4}$$

Thus the relevant magnification factor is 3^a. Moreover, from the discussion in the paragraph before the preceding one, we see that the secondary lines at any stage have the same intensity, while the tertiary ones have a second common intensity.

A final interesting point is that the self-similar spectra described in the preceding paragraph are themselves fractal. At a resolution of Δ_m one anticipates a number of distinguishable lines

proportional to the number of H-atoms in an m^{th} stage gasket, this later number being $\sim 6^m$, as we may recall from (2.2). Thence the spectral fractal dimension should be

$$d_s = \lim_{m\to\infty} \frac{\ln \eta_m}{-\ln \Delta_m} = \frac{ln6}{ln3^a} = d/a$$

That is, it is simply a fraction of the structural fractal dimension d, of (2.13). For the dipolar case of a=3, this gives $d_s \approx 0.54364$. Such low-dimensional fractals (distributed along a line) are sometimes called[2] "Cantor dusts". The present Cantor dust "spreads out" more if a is allowed to decrease toward d. For $a \leq d$ the interaction is in effect long range (there being more perturbative strength due to sites at greater distances) so that the perturbative framework no longer applies. Of course the finer structure of the splitting pattern can also be washed out when it comes to correspond to distances where the effects of sites external to a gasket become comparable to the effect of the intragasket sites (at the same distance).

5. Conclusion

A self-similar sequence of ever more multiply corona-condensed benzenoid species has been investigated with a view to the identification of special characteristics associated to their self-similar character. The Kekulé-structure count and associated resonance-energy estimate seems to behave in a smooth (perhaps unexceptional) fashion. On the other hand excitation spectra for

local modes are argued in a general context to manifest the self-similar molecular structure as a self-similar splitting pattern of the excitation spectra itself. Indeed such local-mode spectra should exhibit their own fractal dimension distinct from (but intimately related to) that of the geometric structure of the molecular gaskets. The identification of other novel features would be of interest.

The self-similar sequence (of figure 2) seems to us a natural one beginning with benzene and coronene, so that the preparation of even just the next member (with over 37 million Kekulé structures) would be an interesting synthetic challenge. We recall Roald Hoffmann's remark that[7] traditional directed (or rational) synthetic organic chemistry has proven successful for quasi-0-dimensional species (i.e., nonextended molecules), less successful for quasi-1-dimensional systems (e.g., thermoplastic polymers), and almost entirely unsuccessful (so far) for 2- or 3-dimensional lattices (such as structurally regular thermosetting polymers or silicates). Amusingly our fractal gaskets may be viewed to offer an intermediate synthetic challenge at intermediate dimensions. Indeed our earlier considerations[3] of possible classical synthetic routes (for another fractal family, exhibiting trigonal symmetry) seem to us to present a circumstance of such an intermediate difficulty.

Finally it can be surmised[3] that fractal benzenoids might serve as zero-order models of various natural carbonaceous substances: coals, lignites, chars and soots. Perhaps those substances can profitably be viewed as having (covalent)

interconnections between aromatic fragments on a range of scales, though the patterns would be randomized and heteroatoms would occur.

It seems there are a variety of rationale for interest in fractal benzenoids and their possible novel properties.

Support of this research is acknowledged to the Welch Foundation of Houston, Texas, and to the Donors of the Petroleum Research Fund administered by the American Chemical Society.

References

1. H. Hosoya, Comp. & Math. Appl. B12 (1986)271-290.

J. L. Bergan, S. J. Cyvin and B. N. Cyvin, Chem. Phys. Lett. 125(1986)218-220.

D. Babić and A. Graovac, Croat. Chim. Acta 59(1986)731-744.

B. N. Cyvin, S. J. Cyvin and J. Brunvoll, Monat. Chemie 119(1988)563-569.

2. B. Mandelbrot, The Fractal Geometry of Nature (W. H. Freeman, San Francisco, 1983).

3. D. J. Klein, M. J. Cravey and G. E. Hite, Polycyclic Aromatic Compounds 2 (1991)163-182.

4. P. G. Carter, Trans. Faraday Soc. 45(1949)597-602.

R. Swinbourne-Sheldrake, W. C. Herndon and I. Gutman, Tetrahedron Lett. (1975)755.

W. A. Seitz, D. J. Klein, T. G. Schmalz, and M. A. García-Bach, Chem. Phys. Lett. 115(1986)139-143.

5. D. J. Klein, G. E. Hite, W. A. Seitz and T. G. Schmalz, Theor. Chim. Acta 69(1986)409-423.

6. S. Alexander and R. Orbach, J. Physique-Lett. 43(1982)L-625.

E. Courtens and R. Bacher, Proc. Roy. Soc. (London) A423(1989)55-70.

7. R. Hoffmann